

The Effect of Addition of Poly(propylene-g-acrylic acid) on the Morphology of Poly(vinyl methylether) and Isotactic Polypropylene Blend

Dong Wang, Hatsuo Ishida

Department of Macromolecular Science and Engineering, Case Western Reserve University, Cleveland, Ohio 44106-7202

Received 8 February 2005; accepted 18 August 2005

DOI 10.1002/app.23429

Published online in Wiley InterScience (www.interscience.wiley.com).

ABSTRACT: The interfacial adhesion of blend of isotactic polypropylene/poly(vinyl methylether) (i-PP/PVME) has been improved by the addition of poly(propylene-g-acrylic acid) (PP-g-AA) as a compatibilizing agent. The phase morphologies of the blends are investigated by optical microscopy (OM) and lateral force microscopy (LFM). The i-PP/PVME (80/20) blend with no addition of PP-g-AA from extrusion process shows a coarse morphology with the dispersed domain size as large as several micrometers; After the addition of 2.5% PP-g-AA in the blends, the dispersed PVME domain size decreases greatly. The addition of 5% PP-g-AA results in a homogeneous morphology. The blend-

ing of PP-g-AA with PVME reduces the crystallization temperature of PP-g-AA, which is different from that of blending i-PP with PVME. The increase of the interfacial adhesion is attributed to the specific intermolecular interaction between the acrylic acid group of PP-g-AA and the ether group of PVME. The specific interaction is studied by Fourier transform infrared spectroscopy. © 2006 Wiley Periodicals, Inc. *J Appl Polym Sci* 101: 4098–4103, 2006

Key words: poly(vinyl methylether); isotactic polypropylene; blend; lateral force microscopy; polypropylene-g-acrylic acid

INTRODUCTION

Polymer blend¹ has drawn great attention in the past 20 years as it is considered to be a convenient and versatile way for the development of new materials with improved properties. However, property improvements are usually dependent on the compatibility of those components. Low compatibility blends usually have coarse phase morphologies and poor adhesion at the interface. To improve the compatibility, so-called compatibilizing agents are often added to the blends to decrease the interfacial tension and achieve more homogeneous dispersion with smaller domain size. Another study of ours² has demonstrated that the preparation conditions could greatly influence phase morphologies and properties of isotactic polypropylene/poly(vinyl methylether) (i-PP/PVME) blends. The blends prepared by casting from a xylene solution at 190°C show homogeneous morphology and the crystallization of i-PP is suppressed by the addition of PVME; whereas the blend from melting extrusion process is phase-separated. The addition of PVME has little effect on the crystallization of PP. The difference was interpreted by the degree of mixing. In

the extrusion blending, those two components could not be mixed well because of their viscosity difference and the weak intermolecular interactions.

As the melt extrusion blending is practically more economical and commonly used, it is important to improve the phase morphology of this blend by extrusion process. In the present article, our research was extended to improving the phase morphology of i-PP/PVME blends from extrusion process by the addition of a small amount of polypropylene-g-acrylic acid (PP-g-AA). PP-g-AA has been reported as a compatibilizing or interfacial agent for the blends or composites of several different polymers or fillers with polypropylene, such as polypropylene/liquid-crystal polymer,³ polypropylene/nylon,⁴ polypropylene/acrylonitrile-butadiene-styrene,⁵ polypropylene/poly(ethylene terephthalate),⁶ and polypropylene/Al(OH)₃ composite,⁷ as the acrylic acid group is polar and reactive. However, there has been no report on the compatibilization of i-PP and PVME using PP-g-AA. In the present research, we expect PP-g-AA to have specific interactions with PVME and, therefore, improve the interfacial adhesion between the i-PP and PVME phases. The molecular interaction between PP-g-AA and PVME was analyzed by Fourier transform infrared (FTIR) spectroscopy. Optical microscopy (OM) and lateral force microscopy (LFM) were used to investigate the morphologies of the blends. The melting and crystallization behaviors of the blends were

Correspondence to: H. Ishida (hxi3@case.edu).

characterized by differential scanning calorimetry (DSC).

EXPERIMENTAL

Materials and sample preparation

The PVME used in this study was purchased from Scientific Polymer Products, Inc. It has a weight average molecular weight, M_{wv} , of 90,000. The i-PP with M_{wv} of 250,000 was obtained from Aldrich Chemical Company. The PP-g-AA was a commercial grade (Polybond 1002) supplied by the Uniroyal Chemical Corp. The amount of acrylic acid content is about 6% by weight. Before blending, the PP-g-AA was dissolved in xylene at 130°C and precipitated into acetone followed by vacuum drying. The blends were prepared by mixing the components using a microcompounder (DACA Instrument) at 200°C and 100 rpm for 10 min.

Differential scanning calorimetry

The thermal properties of the blends were investigated by differential scanning calorimetry (DSC), which was performed on a Modulated DSC 2920 (TA Instruments) at a heating or cooling rate of 10°C/min under a nitrogen atmosphere, in the standard mode. The sample was firstly heated to 200°C and maintained at this temperature for 3 min to eliminate the prior thermal history and the second scan was recorded.

Fourier transform infrared spectroscopy

Fourier transform infrared (FTIR) spectra were obtained on a Bomem-Michelson MB 110 FTIR spectrophotometer, which was equipped with a liquid nitrogen-cooled, mercury cadmium telluride (MCT) detector with a specific detectivity, D^* , of $1 \times 10^{10} \text{ cm Hz}^{1/2} \text{ W}^{-1}$. Co-addition of 128 scans was recorded at a resolution of 2 cm^{-1} after 20 min purge with dry nitrogen to minimize water vapor and atmospheric carbon dioxide.

Optical microscopy

The morphology of the blend was analyzed by optical microscopy (OM), with an optical microscope equipped with a hot stage. A thin slice of the blend sample was sandwiched between a microscope slide and a cover glass and inserted in the hot stage. The sample was first heated to 200°C and then cooled to room temperature to investigate *in situ* morphology during the cooling process.

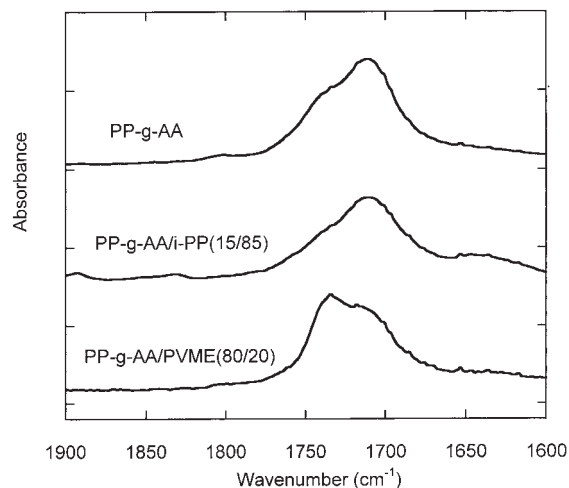


Figure 1 Infrared spectra of plain PP-g-AA, PP-g-AA/i-PP (15/85), and PP-g-AA/PVME (80/20) blends, in the region of 1900–1600 cm^{-1} .

Lateral force microscopy

More details of the morphologies were investigated by lateral force microscopy (LFM). Experiments were performed on a commercial system (Explore, Thermo Microscopes) in contact mode with a spring constant of 0.032 N/m. This type of cantilever was fabricated from silicon nitride (Si_3N_4) and designed in a V-shape with a probe tip integrated onto the underside of the cantilever. The length, width, and thickness of the arm are 200, 18, and 0.6 μm , respectively. The radius of the attached tip is about 20 nm, according to the manufacturer. Imaging was carried out at a repulsive force of 1–2 nN. The deflection and torsion of the cantilever are measured with a four-segment-photo-detector using a laser light irradiating the backside of the free end of the cantilever, which are used, respectively, to obtain topographic and lateral force images. The samples for LFM experiment were prepared by breaking them under liquid nitrogen and the fracture surface was investigated.

RESULTS AND DISCUSSION

Figure 1 shows the infrared spectra of plain PP-g-AA, PP-g-AA/i-PP (15/85) blend and PP-g-AA/PVME (80/20) blends in the region of 1900–1600 cm^{-1} , respectively. For PP-g-AA, two carbonyl stretching bands were observed at 1734 cm^{-1} and 1712 cm^{-1} . The high frequency band is assigned to the free carbonyl stretching and the low frequency band corresponds to the hydrogen bonded C=O in the cyclic acid dimers. The position and relative intensity of the carbonyl band are characteristic of carboxylic acid systems with extensive inter- or intramolecular hydrogen bonding. Comparing to the spectra of poly(acrylic acid) (PAA),⁸

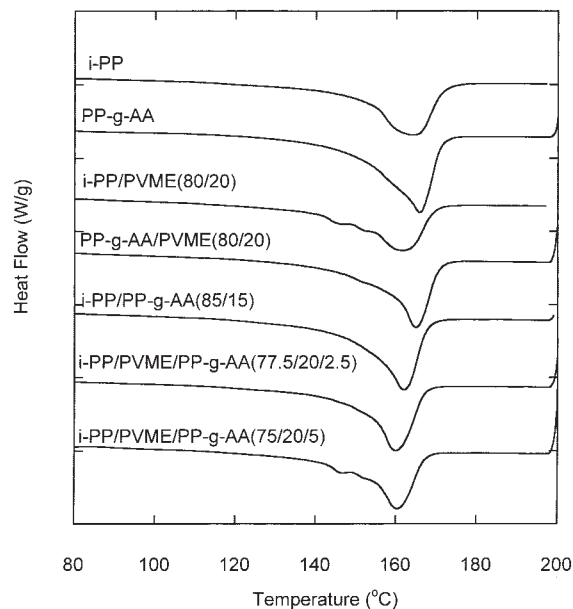


Figure 2 Melting behaviors of i-PP, PP-g-AA homopolymers, and their blends with PVME from the melt extrusion process investigated by DSC at heating rate of 10°C/min.

the relative intensity of the 1734 cm^{-1} band is higher because of the low acrylic acid content per chain compared with PAA. However, the intensity for the band of the hydrogen-bonded C=O group is still higher than the band of free C=O group, indicating that the major acrylic acid groups are in the form of cyclic dimers. The spectrum for the PP-g-AA/i-PP (15/85) blend is similar to that of the neat PP-g-AA, despite the high fraction of i-PP. The little effect of the addition of i-PP on the carbonyl stretching of PP-g-AA suggests that the majority of the hydrogen bonding among the acrylic acid might be intermolecular. On the other hand, upon the blending of PP-g-AA and PVME with PVME content of 15% by weight, the band associated with the cyclic dimers decreases and the intensity for the free C=O group increases significantly. This result indicates change of hydrogen bonds from acid cyclic dimers to acid-ether complexes in the blends of PVME and PP-g-AA, which is consistent with previous results. It has been reported that the interpolymer complex could be formed between PAA and polyether, such as PVME⁸ and poly(ethylene glycol) (PEG).⁹

Figures 2 and 3 show the melting and nonisothermal crystallizations behaviors of i-PP, PP-g-AA homopolymers, and their blends with PVME, respectively, investigated by DSC. PP-g-AA exhibits a similar melting behavior to i-PP, but has a shift of crystallization temperature to higher temperature. As suggested by the literature,¹⁰ the presence of the acrylic acid group could result in enhanced heterogeneous nucleation, leading to the crystallization at a

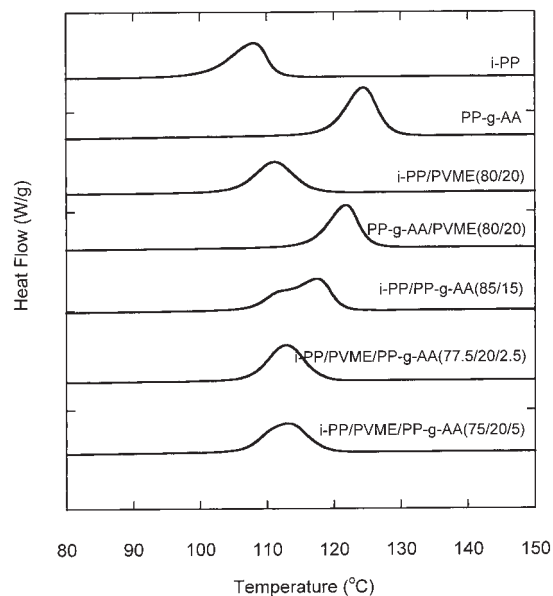
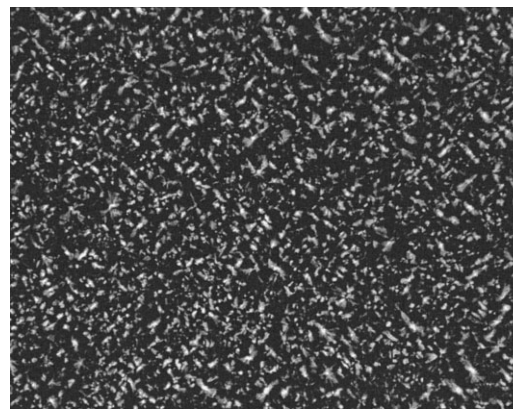
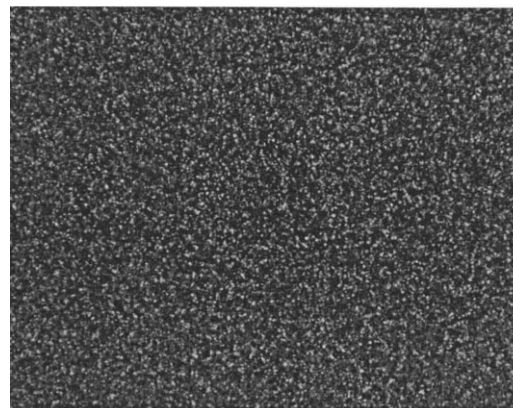


Figure 3 Nonisothermal crystallization behaviors of i-PP, PP-g-AA homopolymers, and their blends from extrusion process with PVME investigated by DSC at cooling rate of 10°C/min.



(a)



(b)

Figure 4 Optical micrographs of i-PP (a) and PP-g-AA (b).

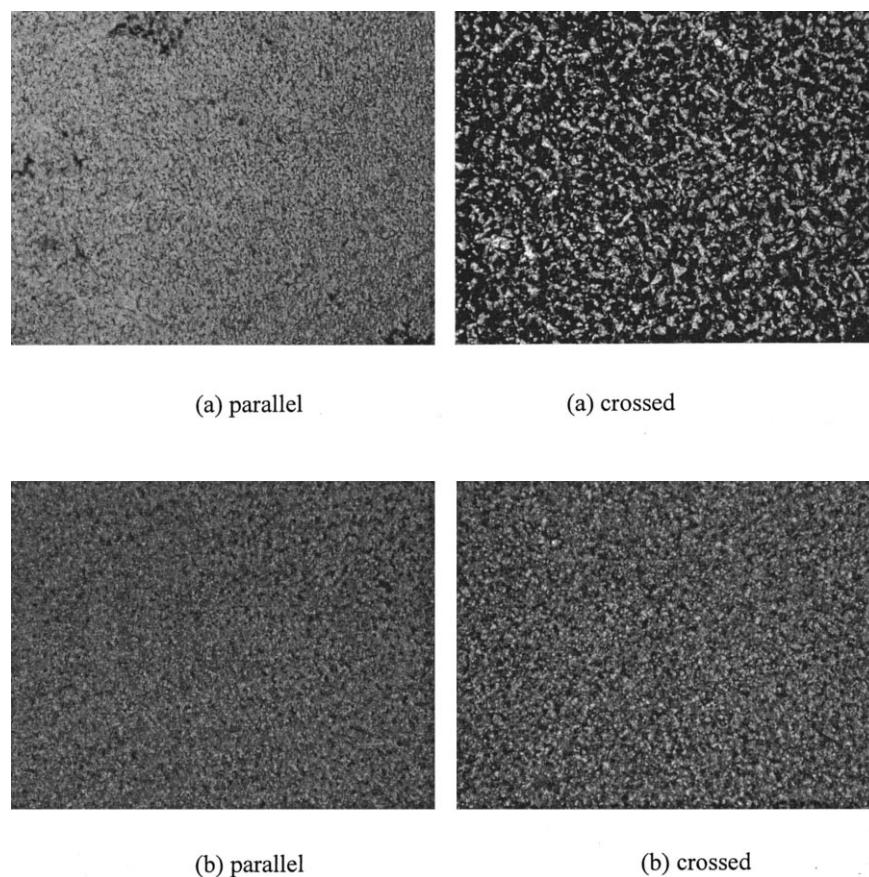


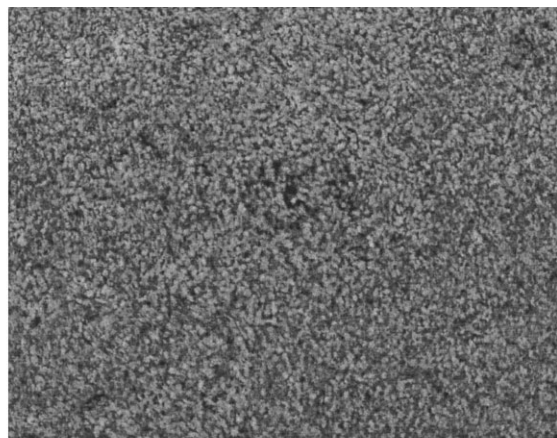
Figure 5 Optical micrographs in parallel and crossed modes, separately, of (a) i-PP/PVME (80/20) and (b) PP-g-AA/PVME (80/20) blends.

higher temperature and the increasing degree of crystallization. This is confirmed by the OM images of PP-g-AA and i-PP as shown in Figure 4. Comparing to i-PP, the size of the spherulite of the PP-g-AA becomes much smaller; indicating the density of crystal nucleus of PP-g-AA is much higher than the neat i-PP. For the i-PP/PP-g-AA (85/15) blend sample, two crystallization peaks, which are between that of pure i-PP and PP-g-AA, arise in the DSC thermogram as shown in Figure 3. This result indicates that PP-g-AA and i-PP might not be totally miscible. Similar to the case of blending of PP-g-AA/i-PP, Cho et al.¹¹ studied the melting and crystallization of the blend of maleic anhydride grafted polypropylene (PP-g-MA) with polypropylene and found that either co-crystallization or phase separation in the blends can be obtained depending on the crystallization conditions. A low cooling rate leads to the phase separation and a high cooling rate results in co-crystallization.

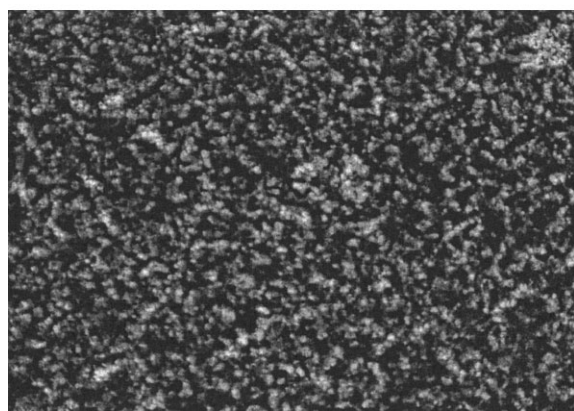
The i-PP/PVME (80/20) blend has similar melting and crystallization behaviors as neat i-PP. Two new melting peaks at lower temperature of about 144°C and 151°C might appear. More details about the blend of i-PP/PVME could be referred in another paper.² On the other hand, although the blending of PVME and

PP-g-AA does not have much effect on the melting behavior of the PP-g-AA, the addition of the PVME resulted in the reduced crystalline temperature of the PP-g-AA as shown in Figure 3, which is different from the effect of blending of i-PP with PVME on the crystallization of i-PP. This difference in the crystallization behaviors should be attributed to the existence of the intermolecular hydrogen bonding between PVME and PP-g-AA as indicated from the FT-IR results shown before. The intermolecular interaction leads to better compatibility of PVME and PP-g-AA with the suppression of both the nucleation and the growth process of the crystallization of PP-g-AA. The better compatibility between PVME and PP-g-AA could be further supported by the OM images as shown in Figure 5. For the i-PP/PVME (80/20) blend sample, the crystallization of i-PP introduces the phase separation, leading to the rejection of the PVME out of i-PP spherulite regions as shown in Figure 5(a). While in the PP-g-AA/PVME (80/20) blend sample [Fig. 5(b)], no obvious phase separation could be observed by OM.

For the i-PP/PVME (80/20) blends with the addition of PP-g-AA with content of 2.5 and 5%, the samples have similar DSC thermograms as those without



(a)



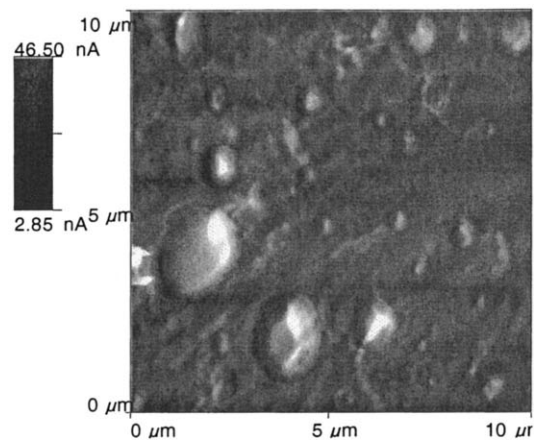
(b)

Figure 6 Optical micrographs in parallel and crossed modes, separately, of i-PP/PVME (80/20) blend with the addition of (a) 2.5% and (b) 5% PP-g-AA.

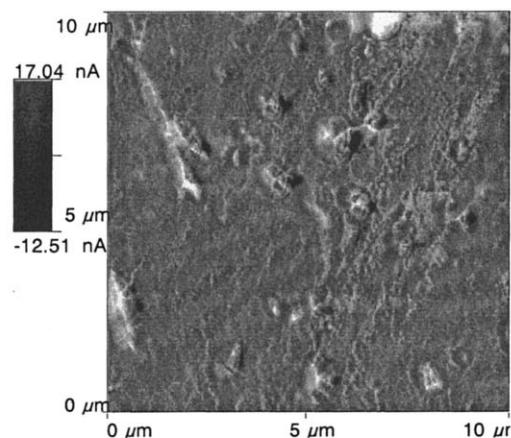
addition of PP-g-AA. On the other hand, Figure 6(a) and 6(b) show the OM images of the i-PP/PVME (80/20) blend with the addition of 2.5 and 5% PP-g-AA, respectively. After addition of PP-g-AA, almost no separation of PVME phase could be resolved by OM. The crystallites of i-PP are more irregular with smaller size compared with the one without addition of PP-g-AA [Fig. 5(a)]. Those brighter crystalline regions might be assigned to the β -crystalline phase of i-PP, which has often been reported for the crystallization of PP-g-AA.¹²

More local morphology details of the blends are investigated by LFM. Figure 7 (a–c) show lateral force (trace) images of the fracture surface of the i-PP/PVME (80/20) blend samples without and with addition of 2.5 and 5% PP-g-AA, respectively. The light contrast areas represent regions of high lateral force, which arise from both friction and the adhesion of the

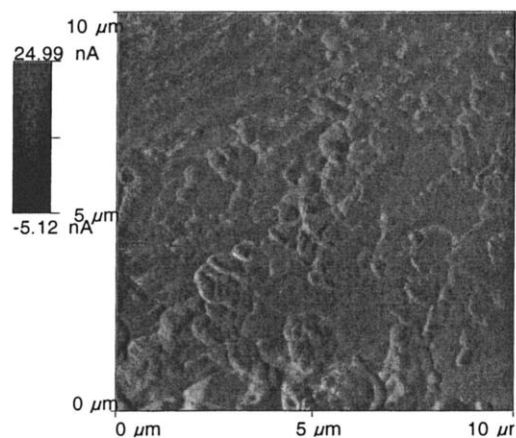
sample,¹³ while the dark contrast areas represent regions with low lateral force. As has been discussed in another paper,² the dark contrast regions in the LFM image are assigned to the i-PP-rich phase and light



(a)



(b)



(c)

Figure 7 LFM images of i-PP/PVME (80/20) blend prepared from melting extrusion. (a) without PP-g-AA; (b) with addition of 2.5% PP-g-AA; (c) with addition of 5% PP-g-AA.

contrast regions are attributed to the PVME-rich phase. As shown in Figure 7(a), the i-PP/PVME (80/20) blend sample with no addition of PP-g-AA shows a coarse morphology with the PVME dispersed in the i-PP matrix. The dispersed domain size could be as large as several microns. After addition of 2.5% PP-g-AA, the domain size of the dispersed phase decreases to only 1–2 μm [Fig. 7(b)]. Compared to the Figure 7(a), the contrast of the lateral force images becomes slightly blurred. A more defused interface between the i-PP-rich region and the PVME-rich phase is observed, indicating a wider concentration gradient of i-PP and PVME due to the increase of the interfacial adhesion. Furthermore, the addition of 5% PP-g-AA results in a much homogeneous morphology with almost no obvious phase separation observed by LFM [Fig. 7(c)]. Therefore, from the OM and LFM results, it is evident that with the addition of the PP-g-AA could improve phase morphologies of the blend i-PP/PVME greatly. These improved phase morphologies could be correlated to the existence of the specific intermolecular interaction between PP-g-AA and PVME as discussed before.

CONCLUSIONS

In the present study, we have shown that there exists the specific intermolecular interaction of the acrylic acid group of the PP-g-AA and ether group of PVME as indicated by the FTIR spectra. The interfacial adhesion of i-PP/PVME blend therefore could be increased

by the addition of small amount of PP-g-AA as a compatibilizer. The addition of 2.5% PP-g-AA reduces the PVME domain size greatly and the addition of 5% PP-g-AA results in a homogeneous morphology. On the other hand, the PVME/PP-g-AA blend shows a better compatibility compared with i-PP/PVME blend and has a suppression of crystallization compared with the plain PP-g-AA.

References

1. Utrachi, L. A. *Polymer Alloys and Blends: Thermodynamics and Rheology*; Hanser: Munich, 1990.
2. Wang, D.; Ishida, H. Case Western Reserve University, unpublished results.
3. Miller, M. M.; Cowie, J. M. G.; Tait, J. G.; Brydon, D. L.; Mather, R. R. *Polymer* 1995, 36, 3107.
4. Lamas, L.; Mendez, G. A.; Muller, A. J.; Pracella, M. *Eur Polym Mater* 1998, 34, 1865.
5. Patel, A. C.; Brahmabhatt, R. B.; Sarawade, B. D.; Devi, S. *J Appl Polym Sci* 2001, 81, 1731.
6. Oromehie, A. R.; Hashemi, S. A.; Meldrum, I. G.; Waters, D. N. *Polym Int* 1997, 42, 117.
7. Mai, K.; Li, Z.; Qiu, Y.; Zeng, H. *J Appl Polym Sci* 2002, 84, 110.
8. Cowie, J. M. G.; Garay, M. T.; Lath, D.; Mceven, L. J. *Br Polym J* 1989, 21, 81.
9. Miyoshi, T.; Takegoshi, K.; Hikichi, K. *Polymer* 1997, 38, 2315.
10. Gallardo, S. G. F.; Valdes, S. S.; Valle, L. F. R. D. *J Appl Polym Sci* 2001, 79, 1497.
11. Cho, K.; Li, F.; Choi, J. *Polymer* 1999, 40, 1719.
12. Rao, G. S. S.; Choudhary, M. S.; Navqvi, M. K.; Rao, K. V. *Eur Polym Mater* 1996, 32, 695.
13. Kajiyama, T.; Tanaka, K.; Takahara, A. *Macromolecules* 1997, 30, 280.